Nanoscale Advances

ROYAL SOCIETY OF CHEMISTRY

PAPER

View Article Online
View Journal | View Issue

Cite this: *Nanoscale Adv.*, 2025, **7**, 4194

UiO-66-NH_2 metal–organic framework supported palladium/Schiff-base complex as a highly efficient and robust catalyst for the Suzuki reaction†

Shiva Kargar and Dawood Elhamifar *

Received 24th January 2025
Accepted 29th May 2025

DOI: 10.1039/d5na00087d

rsc.li/nanoscale-advances

The synthesis of C–C bonds is considered one of the most fundamental challenges in both organic chemistry and the chemical industry, as these bonds are essential for the preparation of high-value products. Therefore, it is crucial to develop efficient, cost-effective, and environmentally sustainable methods for C–C bond formation. In this context, herein, a novel Schiff-base/Pd-functionalized Zr-based UiO-66 MOF (UiO-66/SB-Pd) is synthesized through a straightforward post-modification process and utilized as a highly efficient catalyst in the Suzuki C–C coupling reaction. The designed UiO-66/SB-Pd material was characterized by using FT-IR, EDX, PXRD, TGA, N_2 adsorption–desorption and SEM analyses. This catalyst displayed remarkable catalytic performance and stability in the Suzuki coupling reaction, facilitating the synthesis of a wide range of biaryl compounds. The catalyst retained its activity after seven consecutive cycles. Moreover, a leaching test indicated the excellent stability of the Pd active species under the reaction conditions.

1. Introduction

In recent decades, environmental concerns have driven significant advancements in supported heterogeneous catalysts due to their superior environmental compatibility, enhanced efficiency, and ease of recycling. Metal–organic frameworks (MOFs) are hybrid materials created by the self-assembly of organic linkers and metal cations, attracting considerable interest for their potential in catalysis and other advanced applications.[1–3] MOFs, as porous crystalline coordination polymers, demonstrate distinctive structural and functional properties, such as elevated surface area, remarkable porosity, and variable pore dimensions, in addition to the ability to modify their structure with various organic linkers. These features make MOFs highly attractive heterogeneous catalysts, particularly in organic transformations, where efficient transport and interaction of reactants within the pores enhance catalytic performance.[4,5] Furthermore, MOFs have been extensively employed in diverse applications including gas storage and separation,[6,7] water purification,[8,9] sensing,[10,11] photocatalysis,[12,13] and drug delivery.[14,15] In catalytic systems, MOFs can create acidic or basic sites or serve as a scaffold for other catalysts.[16] Moreover, the catalytic efficacy of functional MOFs can be improved by employing organic linkers *via* post-synthesis modification. Zirconium-based metal–organic frameworks (Zr-MOFs), particularly UiO-66, have garnered significant interest owing to their exceptional hydrothermal stability and diverse uses in catalysis and environmental remediation. UiO-66 is made up of $[Zr_6O_4(OH)_4]$ octahedral secondary building units (SBU) coordinated by 1,4-benzenedicarboxylate linkers.[17–19] The amine-functionalized derivative, UiO-66-NH_2, containing benzene dicarboxylate linkers with attached amine groups, facilitates post-synthetic modifications and offers improved functional characteristics. As a result of these advancements, Zr-MOFs are emerging as powerful platforms for the design of advanced catalytic systems.[20,21] Some recent reports in this matter are UiO-66-NH_2-HPW,[22] UiO-66@Serine,[17] UiO-66-NH_2@cyanuric chloride@2-aminopyrimidine/Pd NPs,[20] UiO-66-N=CH-$C_6H_3PO_4H$,[23] HZSM-5@UIO-66-NH_2/Pd,[24] and UiO-66-NH_2@Pt@mSiO_2.[25]

Meanwhile, the formation of C–C bonds is considered one of the most fundamental and challenging reactions in organic chemistry.[26–31] The Suzuki coupling is a carbon–carbon cross-coupling reaction between organic halides and organic boron compounds, that widely is employed in the synthesis of natural products, pharmaceuticals, and liquid crystalline materials.[32–38] To date, numerous catalytic systems have been utilized for the Suzuki coupling reaction.[39–44] However, their practical application is limited due to the certain drawbacks such as the use of expensive ligands, as well as tedious workup and product separation. Hence, the development of an environmentally-friendly, highly efficient, and affordable catalytic system for the Suzuki coupling reaction is a significant challenge between chemists.

In this work, we report the synthesis and characterization of a novel Zr-based UiO-66 MOF supported Schiff-base/Pd complex (UiO-66/SB-Pd) as well as its catalytic performance in the Suzuki coupling reaction.

Department of Chemistry, Yasouj University, Yasouj, 75918-74831, Iran. E-mail: d.elhamifar@yu.ac.ir

† Electronic supplementary information (ESI) available. See DOI: https://doi.org/10.1039/d5na00087d

2. Experimental section

2.1. Synthesis of UiO-66-NH_2 MOF

UiO-66-NH_2 was synthesized using the same procedure based on the previous work with some modifications.[45] In a typical procedure, 40 mL of DMF was used to dissolve 0.233 g of $ZrCl_4$ and 0.181 g of 2-aminoterephthalic acid (ATA). The mixture was then allowed to agitate at 25 °C for 2 h. Subsequently, the solution was transferred into a 100 mL Teflon-lined stainless-steel autoclave for solvothermal treatment (120 °C, 24 h). The resulting sample was collected by centrifugation after cooling naturally, and it was repeatedly washed with fresh DMF and methanol. Consequently, it was allowed to soak in methanol at 70 °C for an additional 24 h. The resultant pale-yellow product was dried at 100 °C for 12 h and denoted as UiO-66-NH_2.

2.2. Synthesis of UiO-66/SB

To achieve this, the UiO-66-NH_2 (0.5 g) was dispersed in 30 mL of dry toluene at 25 °C for 30 min. Then, salicylaldehyde (2 mL) was added to the reaction vessel and it was allowed to reflux for 24 h. Following centrifugation, the resultant UiO-66/SB was washed with dry EtOH and allowed to dry for 7 h at 80 °C. The solid product was denoted as UiO-66/SB.

2.3. Synthesis of UiO-66/SB-Pd

For this, 0.5 g of UiO-66/SB was dispersed in 20 mL of dry EtOH for 30 min. Then, 1 mmol of $Pd(OAc)_2$ was added and the reaction vessel was agitated at room temperature for 24 h. Following centrifugation, the final product was washed with dry ethanol, dried at 60 °C for 7 h and denoted as UiO-66/SB-Pd. According to the inductively coupled plasma (ICP) analysis the loading of palladium on UiO-66/SB was found to be 0.018 mmol Pd per g.

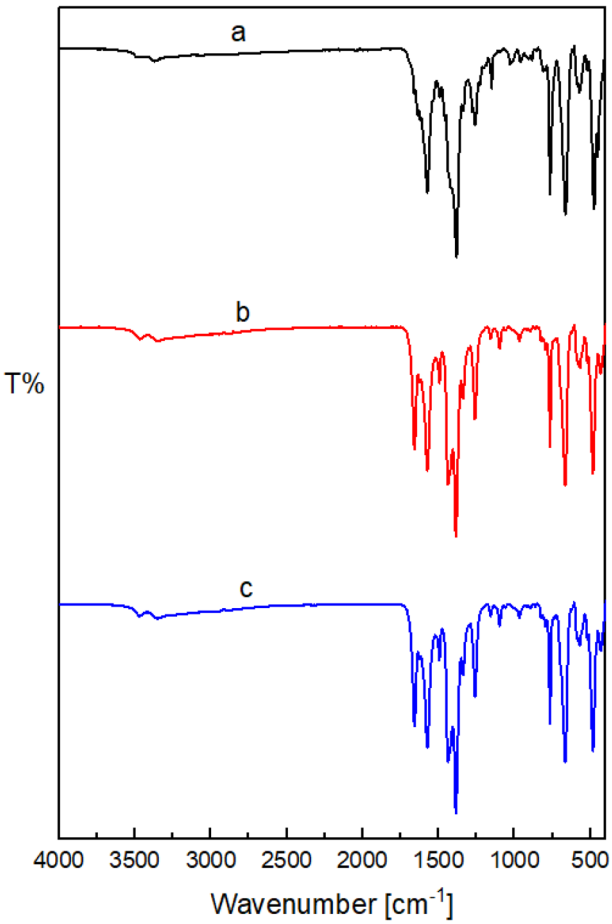

Fig. 1 FT-IR spectra of UiO-66-NH_2 (a), UiO-66/SB (b) and UiO-66/SB-Pd (c).

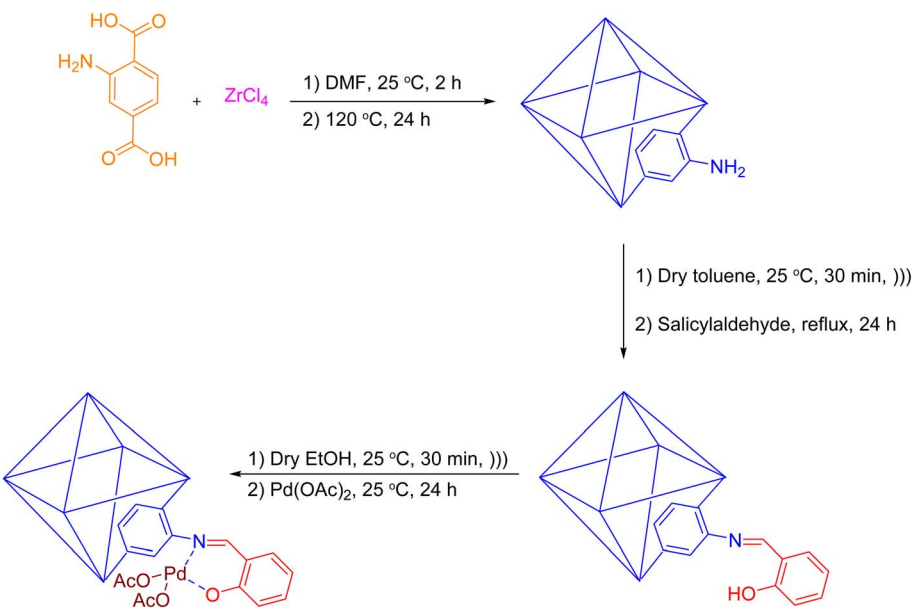

Scheme 1 Preparation of UiO-66/SB-Pd.

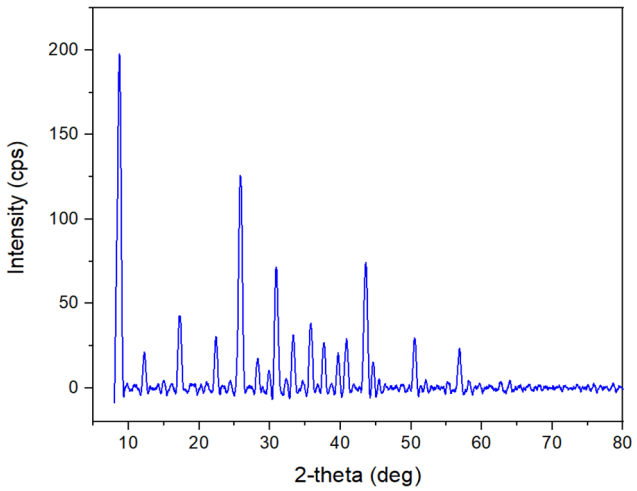

Fig. 2 PXRD of UiO-66/SB-Pd.

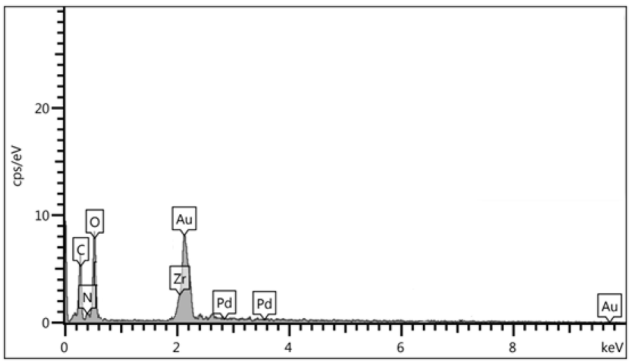

Fig. 3 EDX spectrum of UiO-66/SB-Pd.

2.4. Procedure for the Suzuki cross-coupling using UiO-66/SB-Pd

To carry out the reaction, aryl halide (1 mmol), arylboronic acid (1.5 mmol), K_2CO_3 (2 mmol) and 0.01 g of UiO-66/SB-Pd were added into a reaction flask containing EtOH (10 mL) and the obtained mixture was stirred at 50 °C. After the reaction was finished, the UiO-66/SB-Pd catalyst was removed *via* centrifugation. The purification of the products was accomplished through column chromatography on silica gel using EtOAc and hexane solvents.

2.5. IR and NMR data of some Suzuki products

2.5.1. 4-Phenylbenzaldehyde. IR (KBr, cm^{-1}): 3035 (=C–H, stretching vibration sp^2), 1711 (C=O, stretching vibration), 1602, 1420 (C=C, Ar stretching vibration sp^2). ^{1}H-NMR (400 MHz, $CDCl_3$): δ (ppm) 7.45 (t, $J = 7.2$ Hz, 1H), 7.52 (t, $J = 6.8$ Hz, 2H), 7.68 (d, $J = 7.2$ Hz, 2H), 7.78 (d, $J = 8.0$ Hz, 2H), 7.98 (d, $J = 8.0$ Hz, 2H), 10.09 (s, 1H). ^{13}C-NMR (100 MHz, $CDCl_3$): δ (ppm) 127.3, 127.6, 128.4, 129.0, 130.2, 135.1, 139.7, 147.2, 191.9.

2.5.2. 4-Methylbiphenyl. IR (KBr, cm^{-1}): 3035 (=C–H, stretching vibration sp^2), 2893 (C–H, stretching vibration sp^3), 1608, 1432 (C=C, Ar stretching sp^2). ^{1}H NMR (400 MHz, $CDCl_3$): δ (ppm) 2.38 (s, 3H), 7.27 (d, $J = 7.5$ Hz, 2H), 7.37 (t, $J = 7.4$ Hz,1H), 7.47 (t, $J = 7.8$ Hz, 2H), 7.50 (d, $J = 8.2$ Hz, 2H), 7.59 (d, $J = 7.5$ Hz, 2H). ^{13}C NMR (100 MHz, $CDCl_3$): δ (ppm) 21.1, 127.1, 127.3, 127.6, 129.3, 129.5, 136.3, 139.1, 141.3.

3. Results and discussion

3.1. Characterization of UiO-66/SB-Pd catalyst

Scheme 1 depicts the synthesis procedure of UiO-66/SB-Pd. Initially, UiO-66-NH_2 was synthesized from $ZrCl_4$ and ATA under solvothermal conditions. The UiO-66-NH_2 was then chemically reacted with salicylaldehyde to afford UiO-66/SB.

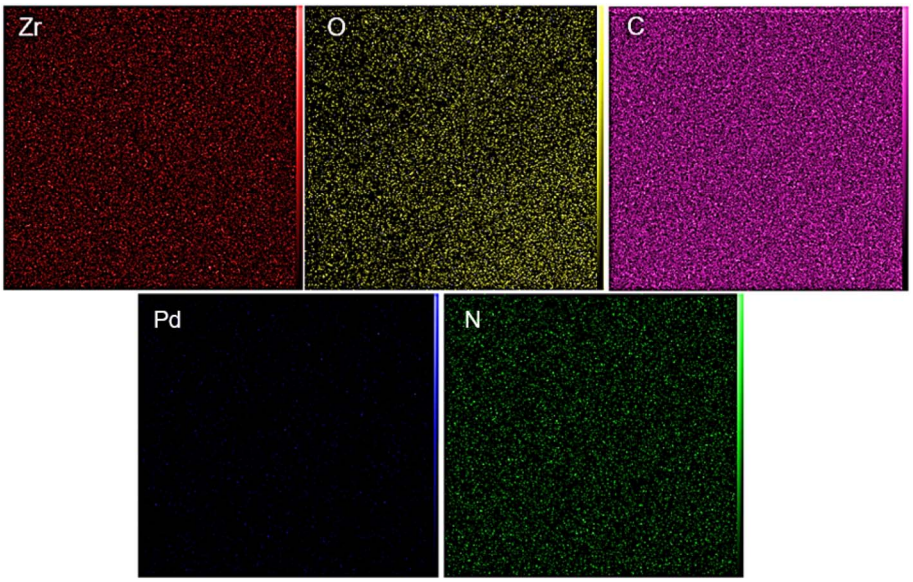

Fig. 4 EDX-mapping of UiO-66/SB-Pd.

The UiO-66/SB-Pd nanocatalyst was finally delivered by treating the UiO-66/SB support with $Pd(OAc)_2$.

Fig. 1 displays the FTIR spectra of the samples at each consecutive stage of the synthesis, including UiO-66-NH_2 (a), UiO-66/SB (b) and UiO-66/SB-Pd (c). The band at 1688 cm^{-1} signifies the stretching vibrations of C=O in carboxylic groups, whereas the strong peaks at 3393 and 3508 cm^{-1} denote the asymmetric vibrations of N–H bonds in the free NH_2 group. The peaks at 1450 and 1594 cm^{-1} indicate the existence of the C=C group in the 1,2,4-substituted benzene ring. The presence of Zr can be confirmed by its distinctive peak at 768 cm^{-1}, associated with the Zr–O stretching vibration.[46] The final UiO-66-NH_2 MOF synthesis is demonstrated by the C=C stretching vibration bands at 1500 cm^{-1}, the symmetric and asymmetric C–O stretching bonds at 1389 and 1568 cm^{-1}, the C–N signals at 1261 and 1346 cm^{-1} and the C–C peak at 1440 cm^{-1} (Fig. 1a).[2,47,48] A successful post-modification was also indicated by the appearance of an imine bond (C=N) stretching vibrations of the Schiff base at 1625 cm^{-1} (Fig. 1b).[49] The observed changes of the C–N and C=N peaks in the UiO-66/SB-Pd catalyst to lower wavenumbers, relative to UiO-66/SB, signify the successful complexation of Pd with the nitrogen atoms of the SB ligand (Fig. 1c).

Powder X-ray diffraction (PXRD) analysis was conducted to examine the crystallinity of UiO-66/SB-Pd (Fig. 2). This analysis displayed diffraction peaks at 2θ values of 8.7°, 14.9°, 17.1°, 22.3°, 25.7°, 30.8°, 32.2°, 35.6°, 37.5°, 40.6°, 43.3°, 50.1°, and 56.9°, which are corresponded to the crystal lattice exhibiting *Fm3m* symmetry of zirconium benzene carboxylate units,[50] indicating that UiO-66-NH_2 retains its high stability throughout the modification processes. It is important to note that the palladium species in the designed catalyst are present as palladium salts rather than as palladium NPs. Accordingly, these NPs are not observed in the PXRD pattern. These results are in good agreement with the previous studies.[51–55]

The immobilization of Pd on UiO-66/SB was investigated by the EDX analysis (Fig. 3). This analysis distinctly confirmed the presence of Zr, O, N, C, and Pd elements in the synthesized material, thereby validating the successful immobilization of the SB/Pd complex on UiO-66-NH_2.

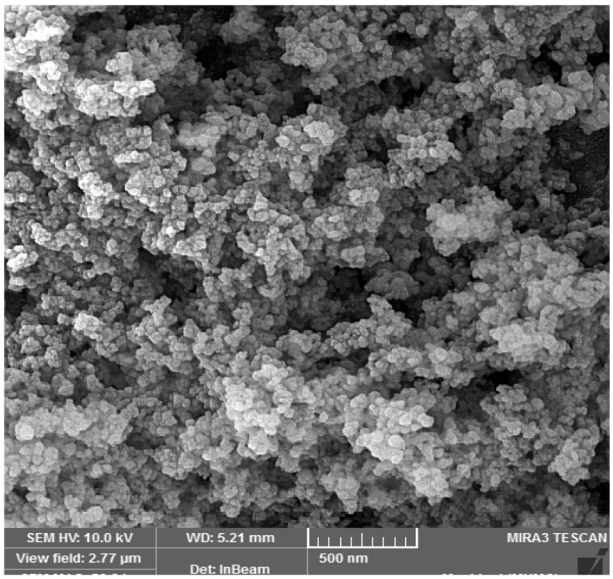

Fig. 6 SEM image of UiO-66/SB-Pd.

Furthermore, the results of the EDX-mapping analysis (Fig. 4), which are consistent with the FT-IR and EDX results, demonstrated that the expected elements are distributed uniformly in the UiO-66/SB-Pd framework.

Thermal gravimetric analysis (TGA) is a crucial method for assessing the composition and thermal stability of materials. Fig. 5 illustrates the TG, derivative TG and heat flow endow down analyses of UiO-66/SB-Pd. The initial weight loss, approximately 3%, occurring below 200 °C is attributed to the

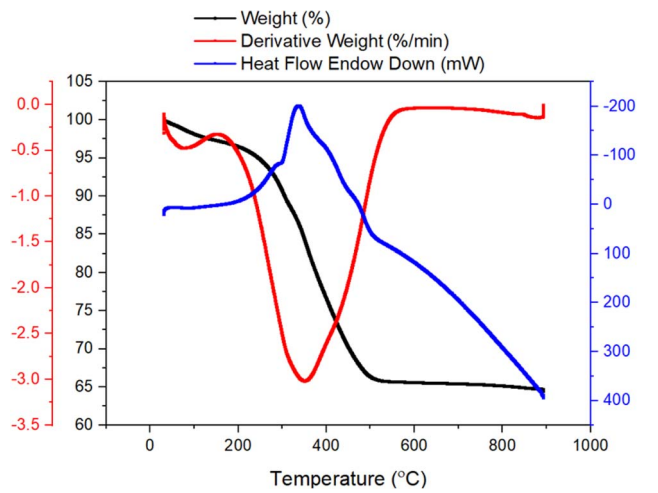

Fig. 5 TG curve of UiO-66/SB-Pd.

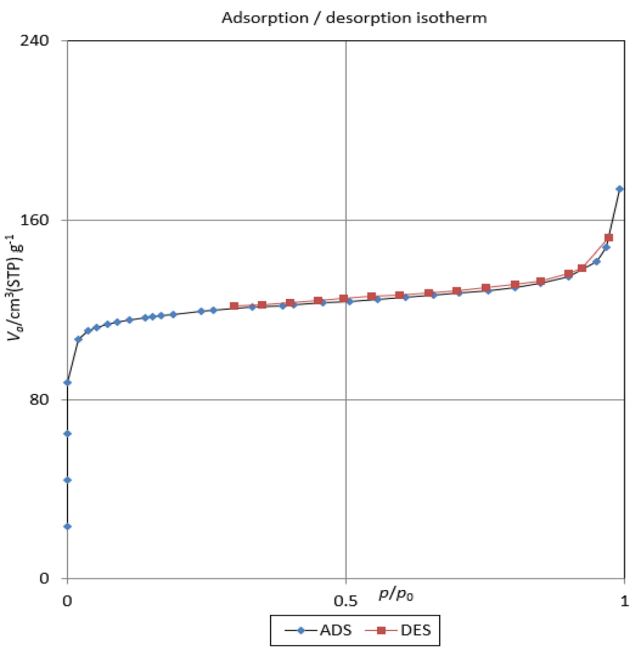

Fig. 7 N_2 adsorption–desorption isotherms of UiO-66/SB-Pd.

evaporation of surface water. The decomposition of DMF is occurred between 200 and 300 °C, and the third weight loss at 300–500 °C could be attributed to the collapse of the UiO-66/SB framework.[3,56] These results demonstrate the exceptional thermal stability of the UiO-66/SB-Pd material.

Scanning electron microscopy (SEM) analysis was employed to examine the morphology and distribution of catalyst (Fig. 6). This illustrates that UiO-66/SB-Pd possesses spherical particles with homogenous distribution.

The specific surface area and porosity of the UiO-66/SB-Pd catalyst were analyzed by N_2 adsorption–desorption measurements at 77 K. As depicted in Fig. 7, the isotherm of UiO-66/SB-Pd shows a typical type I curve with a sharp increase at low pressure areas, demonstrating its microporous properties[57] with a high surface area of 464.3 $m^2\ g^{-1}$.

The BJH pore size distribution analysis indicated that the mean pore diameter of the designed nanocatalyst is 2.28 nm (Fig. 8). The properties such as high specific surface area and the presence of micropores, make these type materials very important candidates for the selective catalytic and adsorption processes.

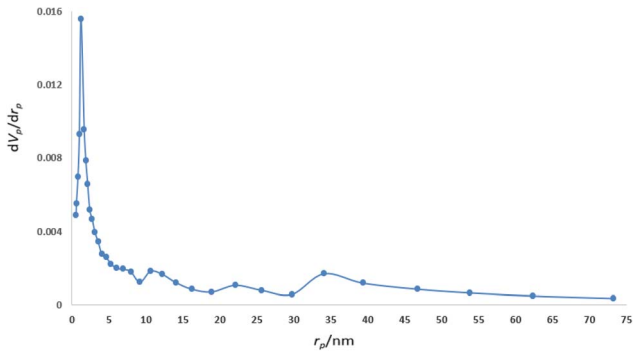

Fig. 8 BJH pore size distribution analysis of UiO-66/SB-Pd.

3.2. Catalytic activity

After a thorough characterization, the performance of UiO-66/SB-Pd was investigated in the Suzuki coupling reaction. In order to find the best conditions for the reaction, the condensation between iodobenzene and phenylboronic acid was selected as a test model. The optimal conditions were determined by evaluating the effects of catalyst amount, temperature, solvent and base. Firstly, the effect of catalyst loading was investigated in the reaction progress. The best product yield was achieved using 0.01 g of the UiO-66/SB-Pd catalyst (Table 1, entry 3). Notably, increasing the catalyst amount to 0.015 g showed no improvement in the reaction yield, while reducing the catalyst amount to 0.005 g led to a significant decline in yield. The effect of temperature was also investigated. This demonstrated that temperature significantly influences the reaction, with the highest conversion achieved at 50 °C. Raising the temperature to 65 °C did not result in any noticeable improvement in the reaction yield (Table 1, entry 3 *vs.* entries 5–7). The effect of various solvents, including H_2O, EtOH, toluene, and MeOH, was also evaluated. The results indicated that H_2O provides the highest yield (97%), whereas toluene gives the lowest product yield (Table 1, entry 3 *vs.* entries 8–10). The reaction sensitivity to different bases was also examined with the results demonstrating that K_2CO_3 exhibited the highest efficiency (Table 1, entry 3 *vs.* entries 11–13). Importantly, the reaction did not occur under base-free conditions. To investigate the role of palladium centers in the catalytic process, the performance of Pd-free UiO-66-NH_2 and UiO-66/SB materials

Table 1 Effect of solvent, catalyst loading, base and temperature in the Suzuki reaction

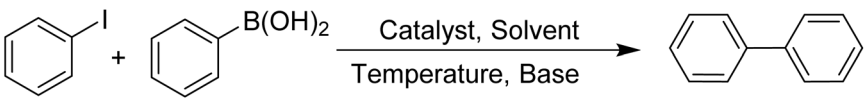

Entry	Catalyst	Cat. loading (g)	Solvent	Temperature (°C)	Base	Time (min)	Yield (%)
1	UIO-66/SB-Pd	0.005	H_2O	50	K_2CO_3	25	47
2	UIO-66/SB-Pd	0.015	H_2O	50	K_2CO_3	25	97
3	**UIO-66/SB-Pd**	**0.01**	**H_2O**	**50**	**K_2CO_3**	**25**	**97**
4	—	—	H_2O	50	K_2CO_3	120	—
5	UIO-66/SB-Pd	0.01	H_2O	25	K_2CO_3	25	55
6	UIO-66/SB-Pd	0.01	H_2O	35	K_2CO_3	25	69
7	UIO-66/SB-Pd	0.01	H_2O	65	K_2CO_3	25	97
8	UIO-66/SB-Pd	0.01	EtOH	50	K_2CO_3	25	86
9	UIO-66-NH_2/SB-Pd	0.01	Toluene	50	K_2CO_3	25	55
10	UIO-66/SB-Pd	0.01	MeOH	50	K_2CO_3	25	88
11	UIO-66/SB-Pd	0.01	H_2O	50	Na_2CO_3	25	82
12	UIO-66/SB-Pd	0.01	H_2O	50	NaOH	25	67
13	UIO-66/SB-Pd	0.01	H_2O	50	NEt_3	25	85
14	UIO-66/SB-Pd	0.01	H_2O	50	—	25	—
15	UIO-66/SB	0.01	H_2O	50	K_2CO_3	25	—
16	UIO-66-NH_2	0.01	H_2O	50	K_2CO_3	25	—

Table 2 Synthesis of Suzuki products in the presence of UiO-66/SB-Pd

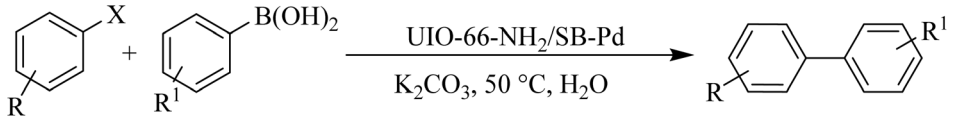

Entry	Aryl halide	Aryl boronic acid	Time (min)	Yield (%)	M. P. (°C)	Reported M. P. (°C)
1	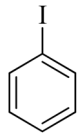	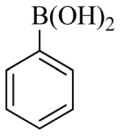	25	97	69–71	68–70 (ref. 58)
2	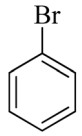	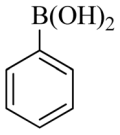	30	91	69–71	68–70 (ref. 58)
3	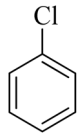	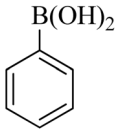	45	84	69–71	68–70 (ref. 58)
4	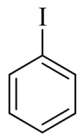	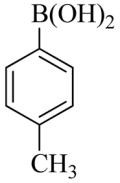	25	96	47–48	46–47 (ref. 58)
5	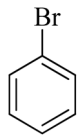	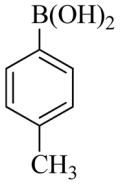	35	94	47–48	46–47 (ref. 58)
6	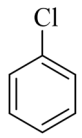	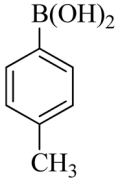	50	83	47–48	46–47 (ref. 58)
7	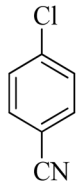	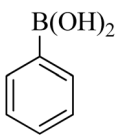	55	88	82–84	83–85 (ref. 26)
8	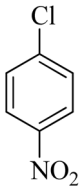	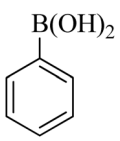	50	92	109–111	110–112 (ref. 26)

Table 2 (*Contd.*)

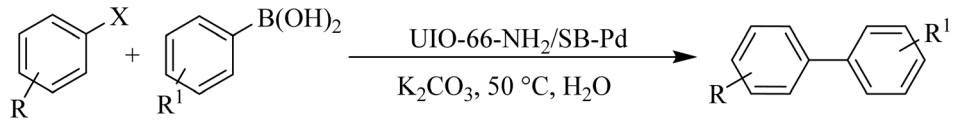

Entry	Aryl halide	Aryl boronic acid	Time (min)	Yield (%)	M. P. (°C)	Reported M. P. (°C)
9	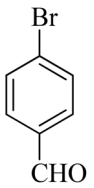	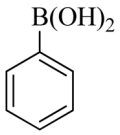	30	94	61–63	59–61 (ref. 26)
10	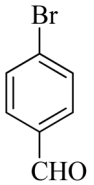	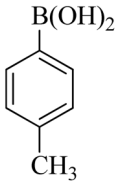	35	95	107–109	106–108 (ref. 26)

was assessed under identical conditions as the UiO-66/SB-Pd catalyst (Table 1, entries 15 and 16). Remarkably, the absence of any conversion or product yield in the presence of these materials highlights the indispensable role of the Pd species in the designed catalytic reaction. Thus, the optimal conditions were determined to be as follows: 0.01 g of UiO-66/SB-Pd catalyst, K_2CO_3 as the base, H_2O as the solvent and a temperature of 50 °C (Table 1, entry 3).

Under optimal conditions (0.01 g of catalyst, H_2O, and 50 °C), the reaction was carried out with various aryl aldehydes to assess the effectiveness of the UiO-66/SB-Pd catalyst. The results demonstrated that all aryl halides give the corresponding biaryl products with high to excellent yields (Table 2). As predicted, the activity of the aryl halides followed the order: aryl iodides > aryl bromides > aryl chlorides. It is also important to note that no detectable homo-coupling byproducts were formed under the applied conditions, further confirming the exceptional efficiency and selectivity of UiO-66/SB-Pd for the cross-coupling reaction.

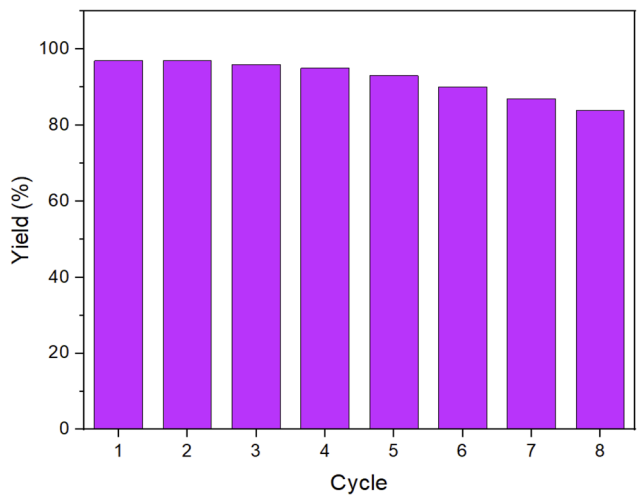

Fig. 9 Recoverability and reusability of the UiO-66/SB-Pd nanocatalyst.

Considering the critical role of catalyst stability in practical applications, the recyclability of the UiO-66/SB-Pd nanocatalyst was evaluated. To do this, after the process was finished, UiO-66/SB-Pd was isolated and reapplied in subsequent runs using identical circumstances as the initial run. It was found that the UiO-66/SB-Pd catalyst is able to maintain its effectiveness for at least seven runs, demonstrating its exceptional longevity in the given conditions (Fig. 9).

The stability of the UiO-66/SB-Pd nanocatalyst under the reaction conditions was assessed by performing a leaching test. To do this, the catalyst was removed from the reaction mixture after achieving a 50% conversion. Then, the reaction of the catalyst-free residue was left to continue for 60 min under applied conditions. Notably, the absence of a significant increase in conversion confirms the heterogeneous nature of the designed catalyst. Moreover, the atomic absorption (AA) spectroscopy showed no leaching of active Pd species in the residue.

In the next study, the performance of UiO-66/SB-Pd was compared to other previously reported catalytic systems used in the Suzuki coupling reaction (Table 3). The results revealed that our catalyst provides significant advantages regarding reaction temperature, catalyst loading, and recyclability. These

Table 3 Comparative study of the efficiency of UiO-66/SB-Pd with the former catalysts in the Suzuki reaction[a]

Entry	Catalyst	Conditions	Time	Recovery times	Ref.
1	KCC-1-NH_2/Pd	Cat. (0.5 mol%), EtOH/H_2O, K_3PO_4, 100 °C	4 h	7	59
2	IL@SBA-15-Pd	Cat. (0.05 mol%), H_2O, K_3PO_4, TBAB, 60 °C	4 h	4	60
3	Pd@CC-SO_3-NH_2	Cat. (10 wt%), H_2O, K_2CO_3, 100 °C	2 h	5	61
4	Fe_3O_4@SiO_2/isoniazide/Pd	Cat. (0.2 mol%), 50 °C, K_2CO_3, EtOH–H_2O	30 min	7	62
5	Pd@CuBDC/Py-SI	Cat. (0.25 mol%), DMF/H_2O, K_2CO_3, 80 °C	1 h	7	63
6	PA–Pd4	Cat. (2 mol%), H_2O, K_2CO_3, 100 °C	1 h	5	64
7	Pd@MC	Cat. (2 mol%), EtOH/H_2O, Na_2 CO_3, 80 °C	1 h	3	65
8	γ-Fe_2O_3-acetamidine-Pd	Cat. (0.12 mol%), DMF, Et_3N, 100 °C	30 min	5	66
9	Pd@[Ni(H_2BDP–SO_3)$_2$	^{i}PrOH/H_2O, K_2CO_3, 60 °C	4 h	4	67
10	Au-graphene	Cat. (1 mol%), H_2O, NaOH, 100 °C	4 h	5	68
11	UiO-66/SB-Pd	Cat. (0.01 g), H_2O, K_2CO_3, 50 °C	25 min	7	This work

[a] Abbreviations: KCC-1: fibrous nano-silica, IL: 1-butyl-3-methylimidazolium hexafluorophosphate ionic liquid, BDC: benzene-1,4-dicarboxylate, Py-SI: pyridyl-salicylimine, PA: polyaniline, MC: mesoporous carbon

outcomes highlight the high efficiency, stability, and durability of the designed catalyst.

4. Conclusion

In summary, a novel UiO-66 MOF supported Schiff-base/Pd complex (UiO-66/SB-Pd) was successfully synthesized using a post-modification approach. The structural morphology and physicochemical properties of the material were investigated using various instrumental techniques. The FT-IR and EDX investigations clearly showed that the Schiff-base/Pd complex is effectively immobilized onto the material network. The SEM image of the designed nanocatalyst revealed well-defined spherical particles of the nanomaterial. The UiO-66/SB-Pd catalyst proved to be an efficient and highly recoverable catalyst for the Suzuki coupling reaction, giving the desired products in high yield at short reaction times and under mild conditions.

Data availability

All data and materials are included in the manuscript.

Conflicts of interest

There are no conflicts to declare.

Acknowledgements

The authors acknowledge Yasouj University and Iran National Science Foundation (INSF) for supporting this work.

References

1 Y.-L. Dong, H.-R. Liu, S.-M. Wang, G.-W. Guan and Q.-Y. Yang, Immobilizing isatin-schiff base complexes in NH2-UiO-66 for highly photocatalytic CO2 reduction, *ACS Catal.*, 2023, **13**, 2547–2554.
2 F. Ghobakhloo, D. Azarifar, M. Mohammadi, H. Keypour and H. Zeynali, Copper (II) Schiff-base complex modified UiO-66-NH2 (Zr) metal–organic framework catalysts for Knoevenagel condensation–Michael addition–cyclization reactions, *Inorg. Chem.*, 2022, **61**, 4825–4841.
3 J. Zhang, Y. Hu, J. Qin, Z. Yang and M. Fu, TiO2-UiO-66-NH2 nanocomposites as efficient photocatalysts for the oxidation of VOCs, *Chem. Eng. J.*, 2020, **385**, 123814.
4 Q. Guan, B. Wang, X. Chai, J. Liu, J. Gu and P. Ning, Comparison of Pd-UiO-66 and Pd-UiO-66-NH2 catalysts performance for phenol hydrogenation in aqueous medium, *Fuel*, 2017, **205**, 130–141.
5 M.-A. Rezaie, A. Khojastehnezhad and A. Shiri, Post-synthetic modification of Zr-based metal organic framework by schiff base zinc complex for catalytic applications in a click reaction, *Sci. Rep.*, 2024, **14**, 24644.
6 H. Daglar, H. C. Gulbalkan, G. Avci, G. O. Aksu, O. F. Altundal, C. Altintas, I. Erucar and S. Keskin, Effect of metal–organic framework (MOF) database selection on the assessment of gas storage and separation potentials of MOFs, *Angew. Chem., Int. Ed.*, 2021, **60**, 7828–7837.
7 H. Li, L. Li, R.-B. Lin, W. Zhou, Z. Zhang, S. Xiang and B. Chen, Porous metal-organic frameworks for gas storage and separation: Status and challenges, *EnergyChem*, 2019, **1**, 100006.
8 C. Chen, L. Fei, B. Wang, J. Xu, B. Li, L. Shen and H. Lin, MOF-based photocatalytic membrane for water purification: a review, *Small*, 2024, **20**, 2305066.
9 W. Zhu, M. Han, D. Kim, Y. Zhang, G. Kwon, J. You, C. Jia and J. Kim, Facile preparation of nanocellulose/Zn-MOF-based catalytic filter for water purification by oxidation process, *Environ. Res.*, 2022, **205**, 112417.
10 Y. Li, M. Xie, X. Zhang, Q. Liu, D. Lin, C. Xu, F. Xie and X. Sun, Co-MOF nanosheet array: A high-performance electrochemical sensor for non-enzymatic glucose detection, *Sens. Actuators, B*, 2019, **278**, 126–132.
11 Z. Zhou, S. Mukherjee, S. Hou, W. Li, M. Elsner and R. A. Fischer, Porphyrinic MOF film for multifaceted electrochemical sensing, *Angew. Chem., Int. Ed.*, 2021, **60**, 20551–20557.

12 Z. Qian, R. Zhang, Y. Xiao, H. Huang, Y. Sun, Y. Chen, T. Ma and X. Sun, Trace to the source: self-tuning of MOF photocatalysts, *Adv. Energy Mater.*, 2023, **13**, 2300086.
13 X. Ma, H. Liu, W. Yang, G. Mao, L. Zheng and H.-L. Jiang, Modulating coordination environment of single-atom catalysts and their proximity to photosensitive units for boosting MOF photocatalysis, *J. Am. Chem. Soc.*, 2021, **143**, 12220–12229.
14 S. Mallakpour, E. Nikkhoo and C. M. Hussain, Application of MOF materials as drug delivery systems for cancer therapy and dermal treatment, *Coord. Chem. Rev.*, 2022, **451**, 214262.
15 E. A. Asl, M. Pooresmaeil and H. Namazi, Chitosan coated MOF/GO nanohybrid as a co-anticancer drug delivery vehicle: synthesis, characterization, and drug delivery application, *Mater. Chem. Phys.*, 2023, **293**, 126933.
16 A. Dhakshinamoorthy and H. Garcia, Catalysis by metal nanoparticles embedded on metal–organic frameworks, *Chem. Soc. Rev.*, 2012, **41**, 5262–5284.
17 F. Ghobakhloo, M. Mohammadi, M. Ghaemi and D. Azarifar, Post-Synthetic Generation of Amino-Acid-Functionalized UiO-66-NH2 Metal–Organic Framework Nanostructures as an Amphoteric Catalyst for Organic Reactions, *ACS Appl. Nano Mater.*, 2024, **7**, 1265–1277.
18 S. Kavak, H. Kulak, H. M. Polat, S. Keskin and A. Uzun, Fast and selective adsorption of methylene blue from water using [BMIM][PF6]-incorporated UiO-66 and NH2-UiO-66, *Cryst. Growth Des.*, 2020, **20**, 3590–3595.
19 A. M. Naseri, M. Zarei, S. Alizadeh, S. Babaee, M. A. Zolfigol, D. Nematollahi, J. Arjomandi and H. Shi, Synthesis and application of [Zr-UiO-66-PDC-SO3H] Cl MOFs to the preparation of dicyanomethylene pyridines *via* chemical and electrochemical methods, *Sci. Rep.*, 2021, **11**, 16817.
20 L. Mohammadi, M. Hosseinifard and M. R. Vaezi, Stabilization of Palladium-Nanoparticle-Decorated Postsynthesis-Modified Zr-UiO-66 MOF as a Reusable Heterogeneous Catalyst in C–C Coupling Reaction, *ACS Omega*, 2023, **8**, 8505–8518.
21 F. M. Moghaddam, A. Jarahiyan, M. Heidarian Haris and A. Pourjavadi, An advancement in the synthesis of nano Pd@ magnetic amine-Functionalized UiO-66-NH2 catalyst for cyanation and O-arylation reactions, *Sci. Rep.*, 2021, **11**, 11387.
22 N. Mulik and V. Bokade, Immobilization of HPW on UiO-66-NH2 MOF as efficient catalyst for synthesis of furfuryl ether and alkyl levulinate as biofuel, *Mol. Catal.*, 2022, **531**, 112689.
23 Z. Karami and M. M. Khodaei, Preparation, characterization, and application of supported phosphate acid on the UiO-66-NH2 as an efficient and bifunctional catalyst for the synthesis of acridines, *Res. Chem. Intermed.*, 2023, **49**, 1545–1561.
24 X. Pan, H. Xu, X. Zhao and H. Zhang, Metal–Organic Framework-Membranized Bicomponent Core–Shell Catalyst HZSM-5@UIO-66-NH2/Pd for CO2 Selective Conversion, *ACS Sustain. Chem. Eng.*, 2020, **8**, 1087–1094.
25 H. Zhao, B. Li, H. Zhao, J. Li, J. Kou, H. Zhu, B. Liu, Z. Li, X. Sun and Z. Dong, Construction of a sandwich-like UiO-66-NH2@Pt@mSiO2 catalyst for one-pot cascade reductive amination of nitrobenzene with benzaldehyde, *J. Colloid Interface Sci.*, 2022, **606**, 1524–1533.
26 S. Kargar and D. Elhamifar, Ionic liquid-containing polyethylene supported palladium: a green, highly efficient and stable catalyst for Suzuki reaction, *Mater. Today Chem.*, 2020, **17**, 100318.
27 M. Dohendou, M. G. Dekamin and D. Namaki, Pd@ l-asparagine–EDTA–chitosan: a highly effective and reusable bio-based and biodegradable catalyst for the Heck cross-coupling reaction under mild conditions, *Nanoscale Adv.*, 2023, **5**, 2621–2638.
28 D. Chakraborty and A. Bhaumik, Advancements in Pd-Based Supported Porous Nanocatalysts for the CC Cross-Coupling Reactions, *Catalysts*, 2024, **15**, 16.
29 M. C. D'Alterio, È. Casals-Cruañas, N. V. Tzouras, G. Talarico, S. P. Nolan and A. Poater, Mechanistic aspects of the palladium-catalyzed Suzuki-Miyaura cross-coupling reaction, *Chem. - Eur. J.*, 2021, **27**, 13481–13493.
30 B. S. Kadu, Suzuki–Miyaura cross coupling reaction: recent advancements in catalysis and organic synthesis, *Catal. Sci. Technol.*, 2021, **11**, 1186–1221.
31 J. J. Boruah and S. P. Das, Palladium (Pd)-based photocatalysts for Suzuki coupling reactions: An overview, *Mini-Rev. Org. Chem.*, 2023, **20**, 687–699.
32 M. Ashraf, M. S. Ahmad, Y. Inomata, N. Ullah, M. N. Tahir and T. Kida, Transition metal nanoparticles as nanocatalysts for Suzuki, Heck and Sonogashira cross-coupling reactions, *Coord. Chem. Rev.*, 2023, **476**, 214928.
33 J. Kouhdareh, H. Keypour, S. Alavinia and A. Maryamabadi, Pd (II)-immobilized on a novel covalent imine framework (COF-BASU1) as an efficient catalyst for asymmetric Suzuki coupling, *J. Mol. Struct.*, 2023, **1273**, 134286.
34 Y. Li, B. Pei, J. Chen, S. Bing, L. Hou, Q. Sun, G. Xu, Z. Yao and L. Zhang, Hollow nanosphere construction of covalent organic frameworks for catalysis:(Pd/C)@ TpPa COFs in Suzuki coupling reaction, *J. Colloid Interface Sci.*, 2021, **591**, 273–280.
35 T. Niwa, Y. Uetake, M. Isoda, T. Takimoto, M. Nakaoka, D. Hashizume, H. Sakurai and T. Hosoya, Lewis acid-mediated Suzuki–Miyaura cross-coupling reaction, *Nat. Catal.*, 2021, **4**, 1080–1088.
36 R. Malav and S. Ray, Carbon-carbon cross coupling reactions assisted by Schiff base complexes of Palladium, cobalt and copper: A brief overview, *Inorg. Chim. Acta*, 2023, **551**, 121478.
37 M. Mora, C. Jimenez-Sanchidrian and J. Rafael Ruiz, Recent advances in the heterogeneous palladium-catalysed Suzuki cross-coupling reaction, *Curr. Org. Chem.*, 2012, **16**, 1128–1150.
38 R. S. Erami, D. Díaz-García, S. Prashar, A. Rodríguez-Diéguez, M. Fajardo, M. Amirnasr and S. Gómez-Ruiz, Suzuki-Miyaura CC coupling reactions catalyzed by supported Pd nanoparticles for the preparation of fluorinated biphenyl derivatives, *Catalysts*, 2017, **7**, 76.
39 H. Veisi, A. Zohrabi, S. A. Kamangar, B. Karmakar, S. G. Saremi, K. Varmira and M. Hamelian, Green

synthesis of Pd/Fe3O4 nanoparticles using Chamomile extract as highly active and recyclable catalyst for Suzuki coupling reaction, *J. Organomet. Chem.*, 2021, **951**, 122005.
40 T. Ben Halima, W. Zhang, I. Yalaoui, X. Hong, Y.-F. Yang, K. N. Houk and S. G. Newman, Palladium-catalyzed Suzuki–Miyaura coupling of aryl esters, *J. Am. Chem. Soc.*, 2017, **139**, 1311–1318.
41 M. Pérez-Lorenzo, Palladium nanoparticles as efficient catalysts for Suzuki cross-coupling reactions, *J. Phys. Chem. Lett.*, 2012, **3**, 167–174.
42 T. Fujihara, S. Yoshida, J. Terao and Y. Tsuji, A triarylphosphine ligand bearing dodeca (ethylene glycol) chains: enhanced efficiency in the palladium-catalyzed Suzuki–Miyaura coupling reaction, *Org. Lett.*, 2009, **11**, 2121–2124.
43 A. Modak, J. Mondal, V. K. Aswal and A. Bhaumik, A new periodic mesoporous organosilica containing diimine-phloroglucinol, Pd (II)-grafting and its excellent catalytic activity and trans-selectivity in C–C coupling reactions, *J. Mater. Chem.*, 2010, **20**, 8099–8106.
44 X. H. Han, K. Gong, X. Huang, J. W. Yang, X. Feng, J. Xie and B. Wang, Syntheses of covalent organic frameworks *via* a one-pot Suzuki coupling and Schiff's base reaction for C2H4/C3H6 separation, *Angew. Chem., Int. Ed.*, 2022, **61**, e202202912.
45 S. P. Tripathy, S. Subudhi, A. Ray, P. Behera, A. Bhaumik and K. Parida, Mixed-Valence Bimetallic Ce/Zr MOF-Based Nanoarchitecture: A Visible-Light-Active Photocatalyst for Ciprofloxacin Degradation and Hydrogen Evolution, *Langmuir*, 2022, **38**, 1766–1780.
46 K. Wang, J. Gu and N. Yin, Efficient removal of Pb (II) and Cd (II) using NH2-functionalized Zr-MOFs *via* rapid microwave-promoted synthesis, *Ind. Eng. Chem. Res.*, 2017, **56**, 1880–1887.
47 M. Kandiah, S. Usseglio, S. Svelle, U. Olsbye, K. P. Lillerud and M. Tilset, Post-synthetic modification of the metal–organic framework compound UiO-66, *J. Mater. Chem.*, 2010, **20**, 9848–9851.
48 F. Zhang, S. Zheng, Q. Xiao, Y. Zhong, W. Zhu, A. Lin and M. S. El-Shall, Synergetic catalysis of palladium nanoparticles encaged within amine-functionalized UiO-66 in the hydrodeoxygenation of vanillin in water, *Green Chem.*, 2016, **18**, 2900–2908.
49 L. Lili, Z. Xin, G. Jinsen and X. Chunming, Engineering metal–organic frameworks immobilize gold catalysts for highly efficient one-pot synthesis of propargylamines, *Green Chem.*, 2012, **14**, 1710–1720.
50 M. Kandiah, M. H. Nilsen, S. Usseglio, S. Jakobsen, U. Olsbye, M. Tilset, C. Larabi, E. A. Quadrelli, F. Bonino and K. P. Lillerud, Synthesis and stability of tagged UiO-66 Zr-MOFs, *Chem. Mater.*, 2010, **22**, 6632–6640.
51 B. Karimi, D. Elhamifar, J. H. Clark and A. J. Hunt, Ordered mesoporous organosilica with ionic-liquid framework: an efficient and reusable support for the palladium-catalyzed suzuki–miyaura coupling reaction in water, *Chem. - Eur. J.*, 2010, **16**, 8047–8053.
52 D. Elhamifar, B. Karimi, J. Rastegar and M. H. Banakar, Palladium-Containing Ionic Liquid-Based Ordered Mesoporous Organosilica: An Efficient and Reusable Catalyst for the Heck Reaction, *ChemCatChem*, 2013, **5**, 2418–2424.
53 M. Neysi and D. Elhamifar, Magnetic ethylene-based periodic mesoporous organosilica supported palladium: An efficient and recoverable nanocatalyst for Suzuki reaction, *Front. Chem.*, 2023, **11**, 1112911.
54 M. Shaker and D. Elhamifar, Core–shell structured magnetic mesoporous silica supported Schiff-base/Pd: an efficacious and reusable nanocatalyst, *New J. Chem.*, 2020, **44**, 3445–3454.
55 M. Neysi and D. Elhamifar, Pd-containing magnetic periodic mesoporous organosilica nanocomposite as an efficient and highly recoverable catalyst, *Sci. Rep.*, 2022, **12**, 7970.
56 H. R. Abid, H. Tian, H.-M. Ang, M. O. Tade, C. E. Buckley and S. Wang, Nanosize Zr-metal organic framework (UiO-66) for hydrogen and carbon dioxide storage, *Chem. Eng. J.*, 2012, **187**, 415–420.
57 Y. Su, Z. Zhang, H. Liu and Y. Wang, Cd0. 2Zn0. 8S@ UiO-66-NH2 nanocomposites as efficient and stable visible-light-driven photocatalyst for H2 evolution and CO2 reduction, *Appl. Catal., B*, 2017, **200**, 448–457.
58 H. Mostafavi, M. R. Islami and A. Momeni Tikdari, Encapsulation of palladium chloride using 2-formylbenzoic acid supported by Fe3O4 nanoparticles modified with SiO2 and propylamine, its characterization and its application for Suzuki coupling reaction, *Appl. Organomet. Chem.*, 2018, **32**, e4384.
59 A. Fihri, D. Cha, M. Bouhrara, N. Almana and V. Polshettiwar, Fibrous Nano-Silica (KCC-1)-Supported Palladium Catalyst: Suzuki Coupling Reactions Under Sustainable Conditions, *ChemSusChem*, 2012, **5**, 85–89.
60 B. Karimi and A. Zamani, SBA-15-functionalized palladium complex partially confined with ionic liquid: an efficient and reusable catalyst system for aqueous-phase Suzuki reaction, *Org. Biomol. Chem.*, 2012, **10**, 4531–4536.
61 P. V. Rathod and V. H. Jadhav, Palladium incorporated on carbonaceous catalyst for Suzuki coupling reaction in water, *Tetrahedron Lett.*, 2017, **58**, 1006–1009.
62 F. Heidari, M. Hekmati and H. Veisi, Magnetically separable and recyclable Fe3O4@SiO2/isoniazide/Pd nanocatalyst for highly efficient synthesis of biaryls by Suzuki coupling reactions, *J. Colloid Interface Sci.*, 2017, **501**, 175–184.
63 S. Rostamnia, H. Alamgholiloo and X. Liu, Pd-grafted open metal site copper-benzene-1, 4-dicarboxylate metal organic frameworks (Cu-BDC MOF's) as promising interfacial catalysts for sustainable Suzuki coupling, *J. Colloid Interface Sci.*, 2016, **469**, 310–317.
64 M. L. Kantam, M. Roy, S. Roy, B. Sreedhar, S. S. Madhavendra, B. M. Choudary and R. L. De, Polyaniline supported palladium catalyzed Suzuki–Miyaura cross-coupling of bromo- and chloroarenes in water, *Tetrahedron*, 2007, **6 13**, 8002–8009.
65 L. Zhong, A. Chokkalingam, W. S. Cha, K. S. Lakhi, X. Su, G. Lawrence and A. Vinu, Pd nanoparticles embedded in

mesoporous carbon: A highly efficient catalyst for Suzuki-Miyaura reaction, *Catal. Today*, 2015, **243**, 195–198.

66 S. Sobhani, M. S. Ghasemzadeh, M. Honarmand and F. Zarifi, Acetamidine–palladium complex immobilized on γ-Fe2O3 nanoparticles: a novel magnetically separable catalyst for Heck and Suzuki coupling reactions, *RSC Adv.*, 2014, **4**, 44166–44174.

67 A. Augustyniak, W. Zawartka, J. Navarro and A. Trzeciak, Palladium nanoparticles supported on a nickel pyrazolate metal organic framework as a catalyst for Suzuki and carbonylative Suzuki couplings, *Dalton Trans.*, 2016, **45**, 13525–13531.

68 Y. Li, X. Fan, J. Qi, J. Ji, S. Wang, G. Zhang and F. Zhang, Gold nanoparticles–graphene hybrids as active catalysts for Suzuki reaction, *Mater. Res. Bull.*, 2010, **45**, 1413–1418.